

BEAM INDUCED DYNAMIC PRESSURE DURING RUN 2 (2015-2018) MACHINE OPERATION IN THE LHC

C. Yin Vallgren*, P. Ribes Metidieri
G. Bregliozzi†, CERN, Geneva, Switzerland

Abstract

The LHC successfully returned to operation in April 2015 after almost 2 years of Long Shutdown 1 (LS1) for various upgrade and consolidation programs. During Run 2 (2015 - 2018) the LHC operated for more than 3600 fills and it has reached a total integrated luminosity of more than 150 fb^{-1} .

This paper summarizes the dynamic vacuum observations in different locations along the LHC during the dedicated fills as well as during the physics runs with different beam parameters. The beam-induced dynamic pressure rise in presence of synchrotron radiation and electron multipacting have been investigated and are presented here. A clear beam conditioning effect has been observed in Run 2.

INTRODUCTION

The LHC vacuum system includes 48 km of cryogenic beam pipes and 6 km of room temperature vacuum system, which were designed to cope with beam dynamic effects, such as electron cloud, synchrotron radiation, impedance heating and ion-induced desorption. The main vacuum pumping system is comprised of cryo-surface pumping, NEG coating pumping and sputter pumps [1].

In this paper, an overview of the evolution of the beam induced pressure rise during Run 2 is given. Run 2 period is considered from April 2015, when the LHC resumed operation after a 2-year period of maintenance (Long Shutdown 1 - LS1), to December 2018, when the LHC operation will be stopped for Long Shutdown 2 - LS2.

Figure 1 shows the schedule for the LHC operation during Run 2 and the upcoming Long Shutdown 2. The different years of operation comprised by Run 2 are separated by 3-month long maintenance closures of the LHC at the end of each year called Year End Technical Stops - YETS (Extended Year End Technical Stops - EYETS if the closure time is 5 months). Each of these periods is followed by a period of recommissioning with beam.

OVERVIEW OF LHC BEAM OPERATION DURING RUN 2 (2015 - OCT 2018)

Figure 2 shows the integrated luminosity during the different years comprised by Run 1 and Run 2 as a function of the date in the corresponding year. In 2015, the integrated luminosity was visibly smaller than in the other operation years mainly due to the shorter operation period after LS1, and an integrated luminosity of 4.24 fb^{-1} and 4.25 fb^{-1} were achieved in ATLAS and CMS, respectively. At the end of

2016 and 2017, integrated luminosities of 38.48 fb^{-1} and 50.82 fb^{-1} were achieved in ATLAS, while luminosities of 40.96 fb^{-1} and 50.58 fb^{-1} were achieved in CMS, respectively at the end of those years. Even though the integrated luminosity during 2018 has only been recorded until October, the curve of integrated luminosity with time shows a steeper slope than previous years and it has already successfully reached a total integrated luminosity of more than 150 fb^{-1} , the set achievement of Run 2.

Table 1 summarizes the achievements and limitations found in during the different years of Run 2.

OVERVIEW OF LHC BEAM PARAMETERS IN RUN 2

LHC beam parameters overview during 2015

The 2015 operations successfully started on the 5th of April under the status of recommissioning with beam. The overview of the LHC beam schedule along the year is summarized in Fig. 3. During 2015 operation, the LHC operated for more than 1000 fills. The 2015 LHC proton physics started with beam of low intensity at 6.5 TeV, followed by two scrubbing runs of high intensity beams at 450 GeV for about 3 weeks, finally ended with 2244 bunches per beam circulating with 25 ns bunch spacing at top energy of 6.5 TeV. The last month of the LHC physics run in 2015 was dedicated to lead ions.

The first scrubbing run started with 50 ns @ 450 GeV on June 24 and finished on July 3. Just after about 24 hours from the start, the 25 ns beam was immediately injected in the LHC. After some struggling with the setting-up of the beams, the LHC was successfully filled with both Beam 1 and Beam 2 consisting of 1020 bunches in trains of 72 bunches with bunch spacing of 25 ns. Beam 2 was strongly limited by the MKI8D degassing leading to pressure close to the interlock's level (5×10^{-8} mbar set by the equipment owner). Measureable vacuum conditioning along most of the LHC was observed. The pressure along the machine did not increase with increasing intensity and were all well below the sector valve interlock thresholds (2×10^{-6} mbar).

Intensity Ramp-up 1, with 50 ns @ 6.5 TeV, was in the end limited to about 450 bunches due to radiation induced faults in Quench Protection System (QPS) electronic boards [2].

The Scrubbing Run 2 continued with the same strategy as the Scrubbing Run 1: inject as many protons as possible into the LHC, in order to create as high as possible electron flux on the inner surfaces of the vacuum chamber and in that way reduce the Secondary Electron Yield (SEY). The first three days were focused on the intensity ramp-up with trains of 72 bunches, followed by 144 bunches from the SPS

* christina.yin.vallgren@cern.ch

† giuseppe.bregliozzi@cern.ch

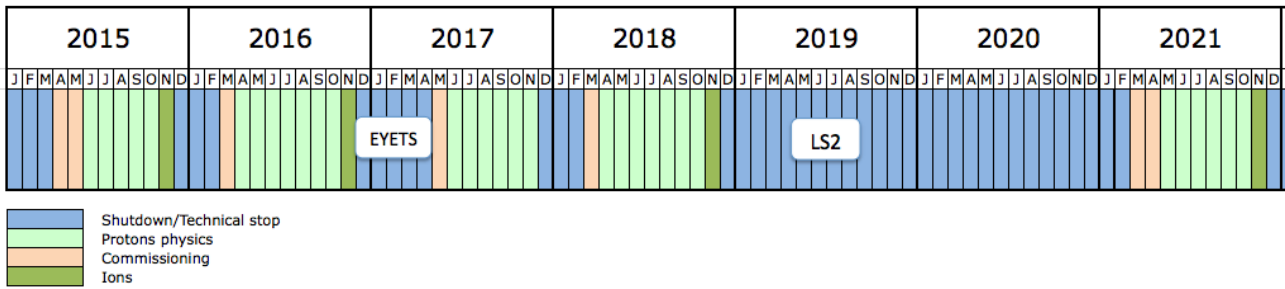


Figure 1: Overview of the LHC beam schedule during Run 2 and LS2.

Table 1: Overview of the operation of the LHC during Run 2.

Year	Top achieved beam intensity [b]	Filling scheme bpi	Limitations
2015	2244	trains of 4x36b	- Limited to 450b by radiation induced faults in QPS electronic boards until TS2. - 144bpi up to 1450b, limited of the available cooling capacity on ARC BS
2016	2220	trains of 96b	Technical issue in the SPS and LHC dumps
2017	2556	trains of 144b	2556b until early August, stable operation with 1900b of 8b4e due to 16L2
2018	2556	trains of 144b	-

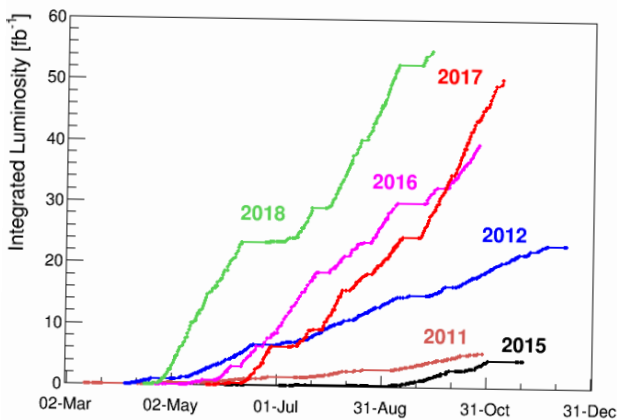


Figure 2: Integrated luminosity during Run 2 (until 01.10.2018).

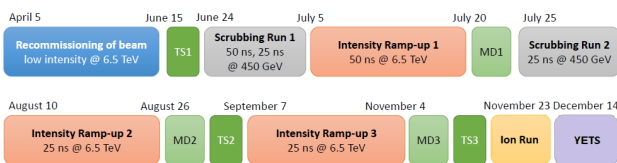


Figure 3: Overview of the LHC beam schedule during 2015.

already on Day 4. The injection process was, in general, slowed down by the cryogenic limitations (to avoid loss of the cryoplant) [3].

In Intensity Ramp-up 3 which was the last physics run with protons before the end of the year, there was one week physics run with high β^* from Oct 12.

The 2015 LHC proton physics ended with 2244 bunches per beam circulating with 25 ns bunch spacing at top energy of 6.5TeV. The first fills consisted of injecting bunch trains of 144 bunches. However, around 1450 bunches, we started approaching the limit of the available cooling capacity on the arc beam screens. The filling schemes changed from 144 bunches train to 72 bunches trains and later 36 bunch trains. The beams with 2244 bunches in total were injected by using the trains of 36 bunches in order not to reach the limitation of the cryoplant. The heat load per bunch significantly decreased by using this strategy.

LHC beam parameters overview during 2016

The 2016 operation successfully started on the 29th March under the status of re-commissioning with beam. The overview of the LHC beam schedule along the year is summarized in Fig.4. During 2016 operation, the LHC operated for more than 800 fills. The 2016 LHC proton physics started with beams of low intensity at 6.5 TeV, without dedicated scrubbing runs. In less than 2 weeks, the LHC already reached 1177 bunches in both beams. Due to the technical limitation in both the SPS and LHC dumps, the beams were limited to 2220 bunches, with 96 bunch train injected from the SPS. The last month of the LHC physics run in 2016 was dedicated to lead ions.

The 2016 LHC proton physics ended with 2220 bunches per beam circulating with 25 ns bunch spacing at top energy of 6.5TeV.

LHC beam parameters overview during 2017

The 2017 operations successfully started on the 1st May under status of re-commissioning with beam, after a 5 months'

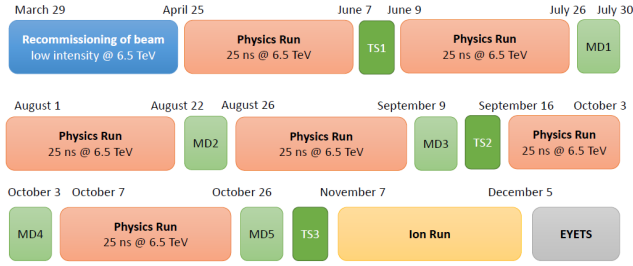


Figure 4: Overview of the LHC beam schedule during 2016.

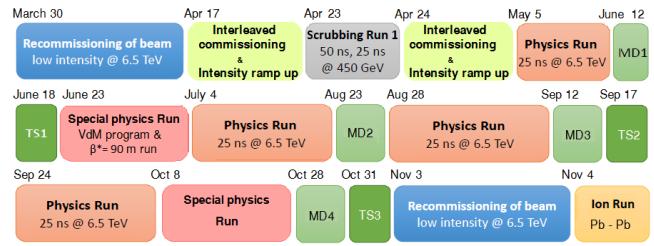


Figure 6: Overview of the LHC beam schedule during 2018.



Figure 5: Overview of the LHC beam schedule during 2017.

period of closure (EYETS). The overview of the LHC beam schedule along the year is summarized in Fig. 5. Even though 2017 was a shorter operational year due to the EYETS, around 150 days of proton physics (including intensity ramp-up) could be ensured, and the LHC operated for more than 800 fills.

The 2017 operation LHC proton physics started with beams of low intensity at 6.5 TeV, after 7 days of dedicated scrubbing at 450 GeV and high intensity. In less than 2 weeks, the LHC already reached 2556 bunches in both beams.

During the last months of operation, a day was dedicated to xenon ions, another day to the VdM run and 16 days were dedicated to a special physics run at 5 TeV and high β^* physics run.

The 2017 LHC proton physics ended with 1868 bunches per beam circulating with 25 ns bunch spacing at top energy of 6.5 TeV due to the so-called *16L2* issue [4] and the special filling scheme with 8b4e type of beam was introduced to avoid the high heat load in some parts of the ARCs.

LHC beam parameters overview during 2018

The 2018 operation started on the 30th of March under the status of recommissioning with beam. The overview of the LHC beam schedule along the year is summarized in Fig.6. During the period from March to July of the 2018 operational year, the LHC has operated for more than 1300 fills.

The 2018 operation LHC proton physics started with beams of low intensity at 6.5 TeV, after 17 days of interleaved commissioning and one day of dedicated scrubbing run.

LHC PRESSURE EVOLUTION DURING RUN 2

In this section, an overview of the average dynamic pressure rise for several specific locations in the LHC with physics beam of 25 ns at 6.5 TeV at stable beam during Run 2 is presented.

LHC Long Straight Sections pressure evolution

Figure 7 shows the average reading of Bayard-Alpert gauges installed ± 100 -120 m from the Interaction Points (IP) in the Combination Chambers (CC) of each Long Straight Section (LSS), where both beams circulate in the same beam pipe and the vacuum chambers are mostly Non-Evaporable Getter (NEG) coated. Because the two beams come from both directions, the effective bunch spacing in these regions can be as low as half of 25 ns. It can be appreciated that during Run 2 the pressure in the studied regions doesn't exceed in any case a value of 10^{-8} mbar, a clear proof for the electron cloud mitigation efficiency of the NEG coatings.

Figure 8 shows the normalized average pressure reading of the same Bayard-Alpert gauges. Between the different operation years in Run 2, it can be observed a pressure *de-conditioning* effect, followed by a fast conditioning. It is also interesting to point out that a slight pressure increase in LSS1 (where the experiment ATLAS is located) and LSS5 (where the experiment CMS is located) can be appreciated in Fig. 8, which could be explained by a partial saturation of NEG in these regions.

Figure 9 summarizes the overview of the average dynamic pressures for special sectors in the LHC, such as for the NEG pilot sectors (dedicated NEG coated sections for studies in IP7, A5R2, A6L8), the cold-warm transitions, where the synchrotron radiation is strongly present, and at the cold-warm transitions, where the synchrotron radiation is negligible, i.e. at injection energy.

It is interesting to notice that as shown in Fig. 9, the pressure in a cold-warm transition in the presence of synchrotron radiation is approximately twice as large as the pressure in the same location at the end of injection, i.e., in the absence of synchrotron radiation.

Figure 10 displays the average dynamic normalized pressures for the NEG pilot sector, for the cold-warm transition with and without the presence of synchrotron radiation. Figure 10 shows a very low pressure in the dedicated NEG

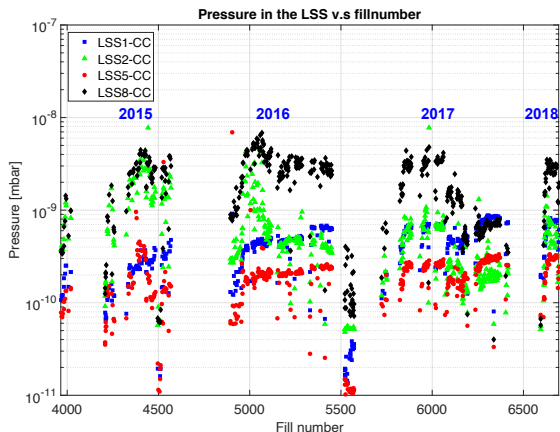


Figure 7: Average reading of Bayard Alpert gauges ± 100 -120 m from IP in the combination chambers (CC) of each LSS.

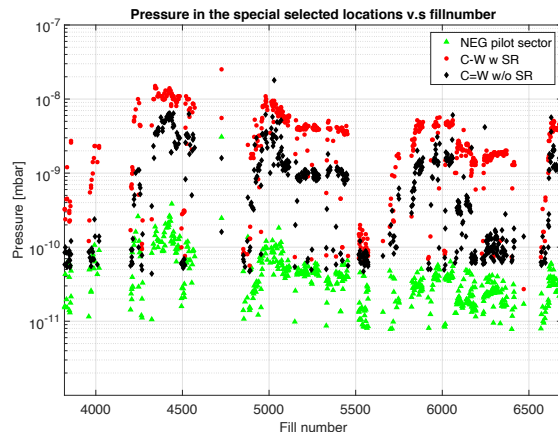


Figure 9: Average dynamic pressure evolution in the NEG pilot sectors, in a cold-warm transitions in the presence and absence of synchrotron radiation.

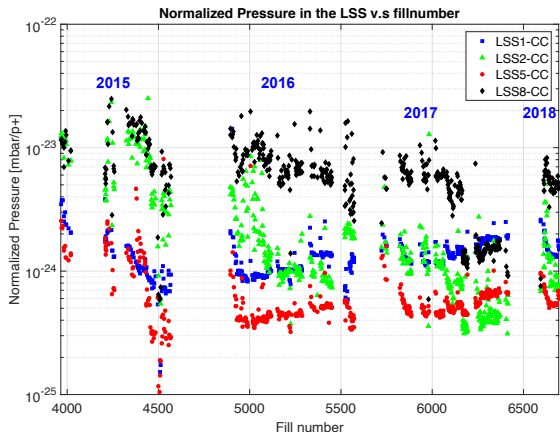


Figure 8: Average reading of Bayard Alpert gauges installed ± 100 -120 m from IP in the combination chambers (CC) of each LSS normalized by the beam intensity.

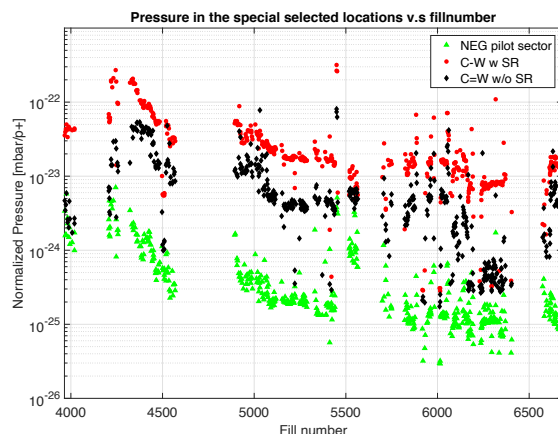


Figure 10: Normalized average dynamic pressure evolution in the NEG pilot sectors, in a cold-warm transitions in the presence and absence of synchrotron radiation.

pilot sector during all Run 2 and no real pressure increase in-between the operation years.

LHC experimental areas' dynamic pressure rise

In this section, pressure as a function of time for a typical physics fill is plotted for ATLAS and CMS experiments and shown in Fig. 11, 12 and 13. A correlation between the dynamic pressure and the beam intensity, beam energies and luminosity is clearly visible. The typical curve in pressure can be divided into three main pressure rise peaks, with a typical example of ATLAS detailed in Fig. 11. The first pressure peak with the maximum at the end of injection indicates the dynamic pressure rise due to electron cloud in the beam pipe. The second pressure peak at the maximum of the beam energy ramp-up indicates the effect of synchrotron radiation from the Inner triplets (IT). The third one well correlates with the luminosity, the same as seen in the case of CMS (Fig. 12). However, the reason for the sudden pressure rise right after the start of collision is not yet clear.

This could be a result of particle lost during or generated by collisions, that desorb gas molecules from the walls. Or this could also be ionization in the cables for the gauges close to the IP area. However, it is worth mentioning that the pressure seems to increase with increasing luminosity. More studies in this area are ongoing. On the other hand, since the collision rate for ALICE and LHCb are comparably smaller, no visible pressure rise is detected after the start of collisions in those experiments (Fig. 14) and Fig. 15).

Figures 12 and 13 show the pressure evolution for two selected fills in CMS. The main difference between the two selected fills is that in fill 4532 the CMS detector solenoid was on and during fill 4536 it was turned off. With and without CMS detector solenoid on, a clear difference in the pressure induced by electron cloud is shown in Fig. 12 and 13, when the beams were injected. The detector seems to have a clear effect on suppressing of the electron cloud in the interaction point of the CMS detector. It is also noted that

the CMS gauge seem to be very sensitive to the electronics interference.

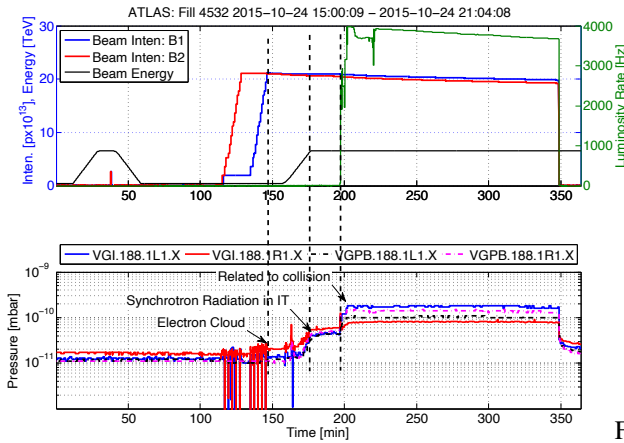


Figure 11: ATLAS Experiment, fill 4532 (1825b).

LHC ARC pressure evolution

The average of the dynamic pressure in the different ARCs as a function of the fill number is shown in Figs. 16 and 18 for beam 1 and 2, respectively. Figure 17 and 19 exhibit the normalized dynamic pressure in the different ARCs as a function of the fill number for beam 1 and 2 respectively.

At the beginning of each operation year of Run 2, the scrubbing runs provided sufficient mitigation against beam-induced pressure rise at 450 GeV. As a consequence, a fast decrease of the dynamic average pressure in the ARCs due to the conditioning effect can be appreciated.

During the physics runs of Run 2, the cooling capacity on the ARC beam screen approached its pre-defined design limit (160 W/half cell). During 2015, sectors 12 and 23 presented the highest heat load, while in 2016 and 2017 the sectors with the highest heat load were 81 and 12. The abrupt

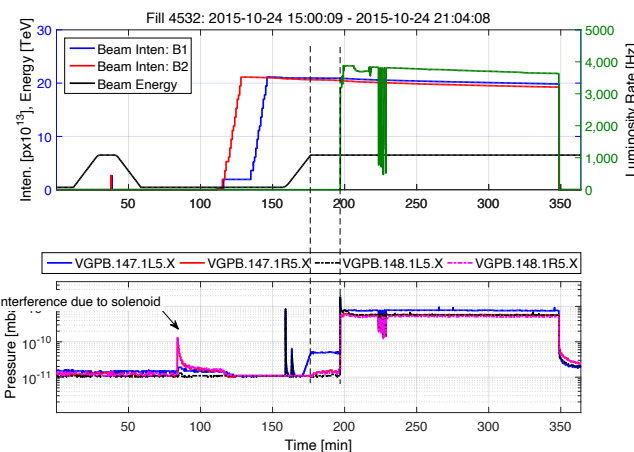


Figure 12: CMS Experiment, fill 4532 (1825b).

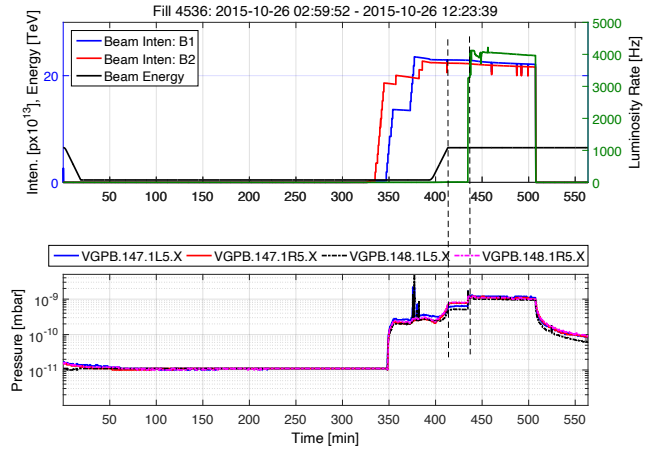


Figure 13: CMS Experiment, fill 4536 (2041b). The CMS detector solenoid was turned off.

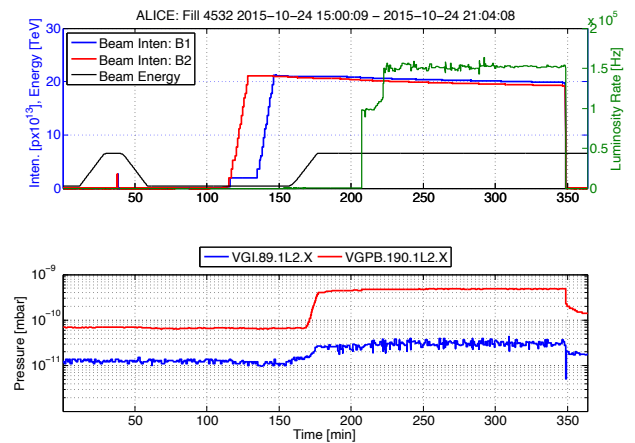


Figure 14: ALICE Experiment, fill 4532 (1825b).

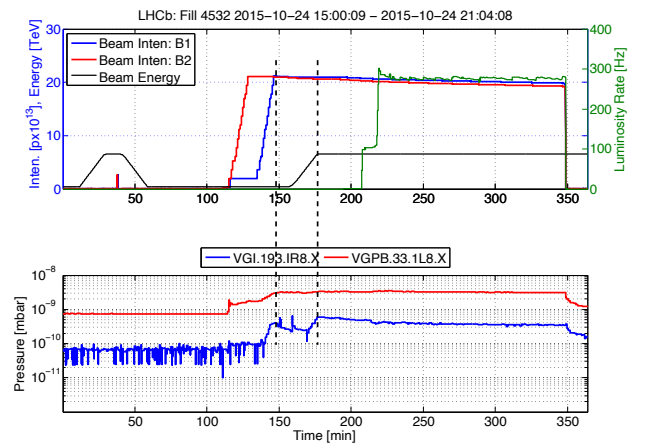


Figure 15: LHCb Experiment, fill 4532 (1825b).

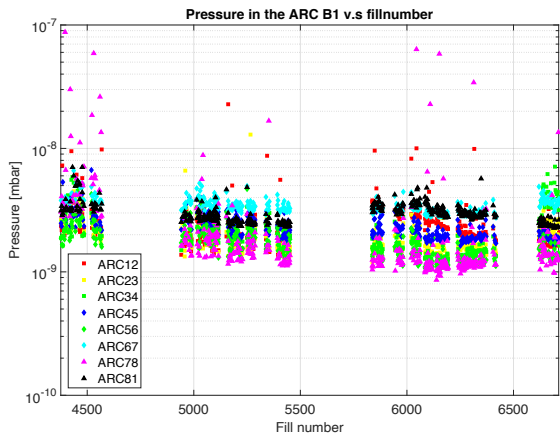


Figure 16: Average of the dynamic pressure in the different ARCs as a function of the fill number for beam 1.

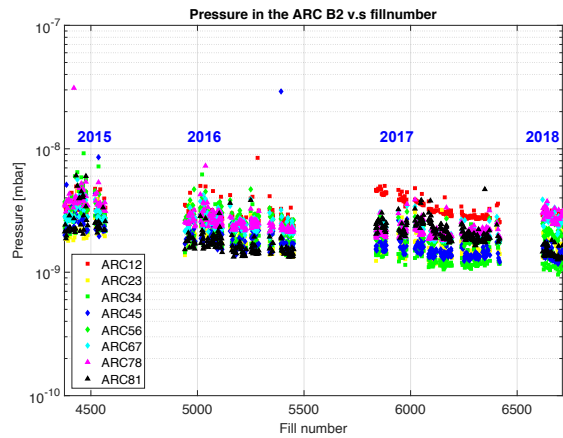


Figure 18: Average of the dynamic pressure in the different ARCs as a function of the fill number for beam 2.

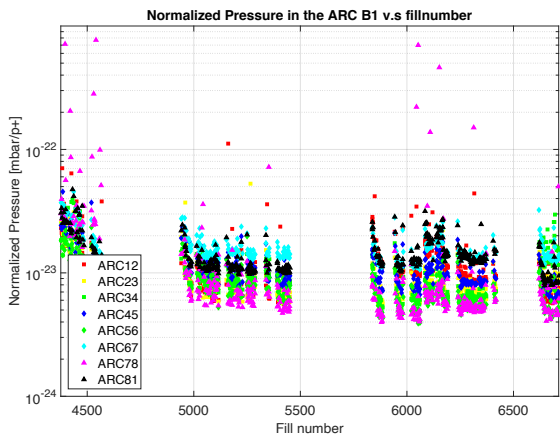


Figure 17: Normalized average dynamic pressure in the different ARCs as a function of the fill number for beam 1.

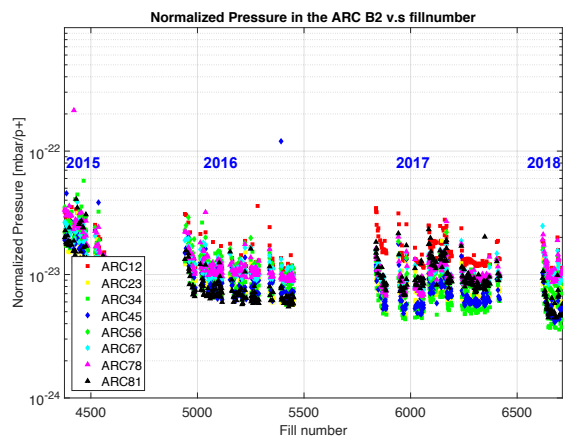


Figure 19: Normalized average dynamic pressure in the different ARCs as a function of the fill number for beam 2.

reduction of the heat load at the end of 2017 corresponds to the introduction of the filling scheme 8b4e.

In term of pressure, different sectors exhibit the highest pressure rise during the operation years of Run2. For beam 1, the sectors with the highest pressure rise during 2015 were ARC 12 and 78, while during 2016, 2017 and 2018, the sectors with the highest pressure rise were ARC 12 and 81. For beam 2, the sector with the highest pressure rise during the entire run was ARC 12. It can also be noted that from the beginning of 2016, the sector with the lower pressure corresponds to ARC 78, whilst the smallest heat load contribution comes from ARC34. For this reason, we can conclude that a clear correlation between high pressure and high heat load can not directly be extracted from these observations.

The scrubbing in the ARCs during the scrubbing run for both 50 ns and 25 ns is sufficient to reduce the pressure rise due to electron cloud, as confirmed in Fig. 22a and 22b. However, after the Technical Stop 2 in 2015 (TS2, a maintenance shutdown for about 5 days), a clear increase

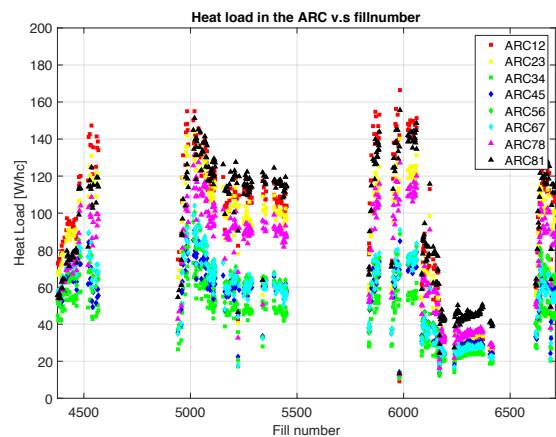


Figure 20: Average heat load in the different ARCs as a function of the fill number.

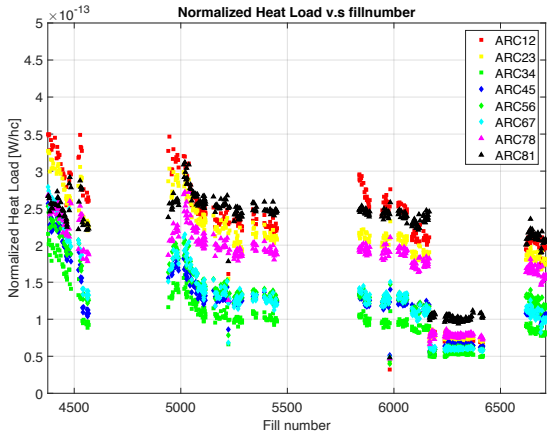


Figure 21: Average normalized heat load in the different ARCs as a function of the fill number.

in pressure was also observed in the ARCs, as shown in Fig. 22c.

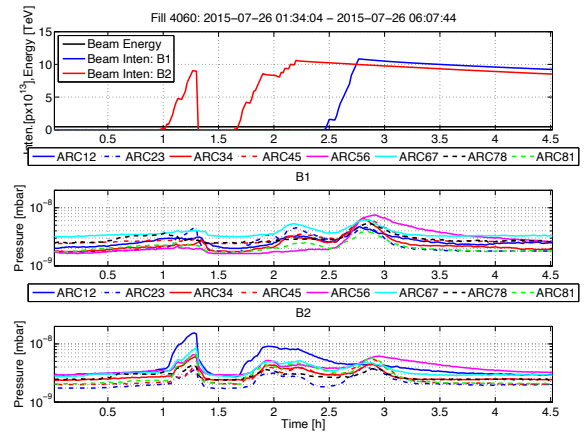
Figure 22c clearly shows the loss of conditioning effect accumulated during Scrubbing Run 2 and Physics Run 2. The reduction of the pressure rise seemed to be reset completely. It is more likely that the loss of conditioning was rather due to the low energy beams circulated in the machine after TS2 than long term in-activities of the beam. De-conditioning was observed mainly when running with low e-cloud filling schemes (Physics Run 2, MD combined with TS, High β^*). Recovery of conditioning was achieved quickly, as shown in Fig. 23.

In order to study the causes of the de-conditioning observed in the LHC, the evolution of the Electron Stimulated Desorption (ESD) yield and of the Secondary Electron Yield (SEY) of fully conditioned copper left under ultra high vacuum (UHV) have been studied and are presented in Fig. 24 and 25, respectively.

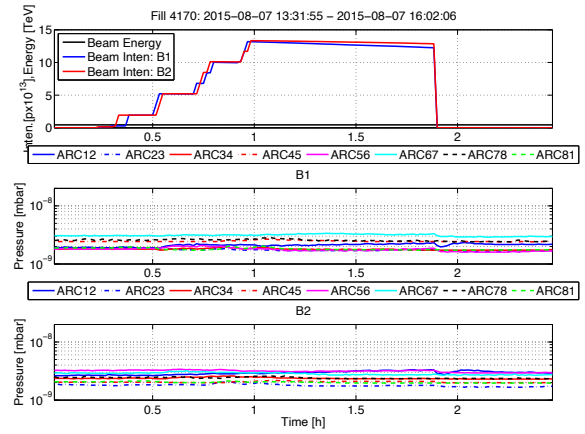
As shown in Fig. 24, after leaving a sample of fully-conditioned copper under ultra high vacuum (UHV) for a week, a noticeable increase of its ESD as a function of the electron dose could not be observed. Similarly, a significant increase in the SEY of fully-conditioned copper left for 16 days under UHV could not be observed either. These results arouse new questions on how the observed pressure rise after a prolonged TS are generated. More studies are ongoing in this topic.

CONCLUSIONS

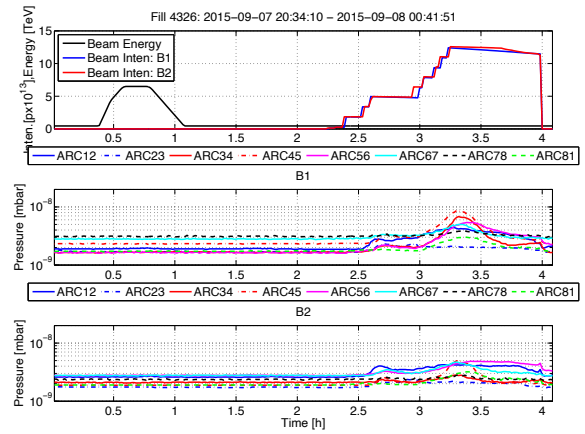
In conclusion, the LHC vacuum performance in Run 2 is overall successful after all the upgrades made during the LS1. The LHC operation was mainly characterized by high heat load in four ARCs and the so-called *16L2* issue, which gives more than 50 unexpected dumps. Understanding the cause of the high heat load in some of the ARC sectors is extremely important for the future operation runs.



(a)



(b)



(c)

Figure 22: 25 ns scrubbing run validation and de-conditioning. Average pressure for each of the ARCs for Beam 1 and 2. (a): Fill 4060, 25 ns, B1:1236b and B2: 1236b. Pressure increase in the ARCs before the 25 ns scrubbing run. (b): Fill 4170, 25 ns, B1: 1176b B2: 1176b. No pressure increase. (c): Fill 4326: same filling scheme as Fill 4170, 25 ns, B1: 1176b B2: 1176b after TS2.

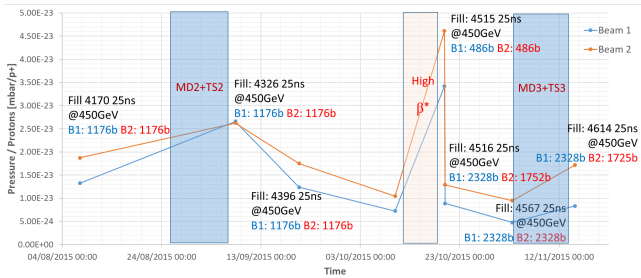


Figure 23: Observed loss of the conditioning effect in pressure in ARCs during the technical stops. Average maximum pressure of each of the ARCs for the selected scrubbing checks @450 GeV.

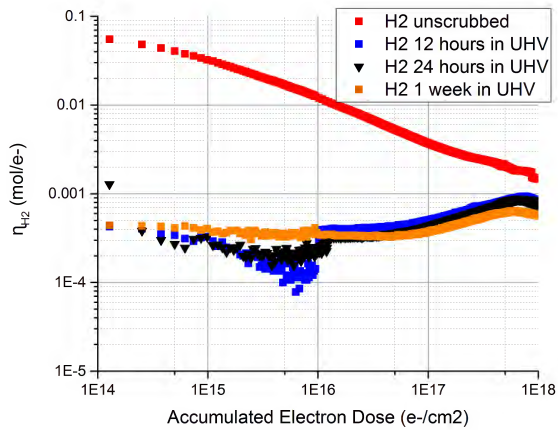


Figure 24: Electron Stimulated desorption (ESD) of backed copper as a function of the accumulated electron dose (courtesy by S. Callegari [5]).

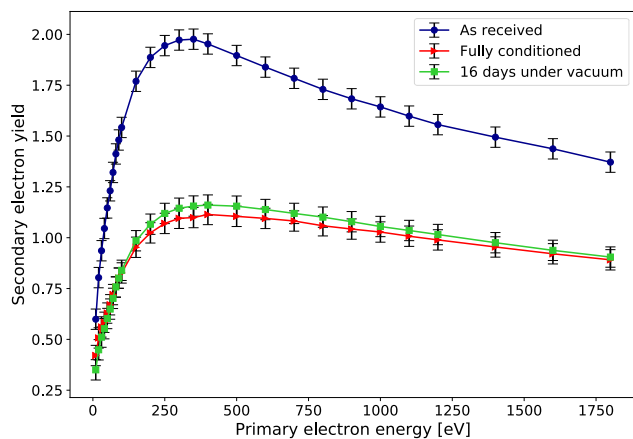


Figure 25: Secondary Electron Yield (SEY) of unbacked copper as a function of the primary electron energy (courtesy by V. Petit).

ACKNOWLEDGMENTS

Special thanks to Simone Callegari and Valentine Petit for contributing with the experimental ESD curves and SEY curves, respectively.

REFERENCES

- [1] J. Jimenez and et al, “Vacuum and cryogenics observations for different bunch spacing,” 2011. Proceedins of Chamonix 2011 workshop on LHC Performance.
- [2] J. Uythoven, “Machine protection at 6.5 TeV.” in Chamonix 2016.
- [3] G. Ferlin, “Cryogenics.” in Chamonix 2016.
- [4] L. Mether, “16L2: Operation, observations and physics aspects.” in Evian 2017.
- [5] S. Callegari and et al, “Electron Stimulated Desorption Studies on Copper After Bake-Out in Ultra-High Vacuum and with Different Venting Conditions.” EVC-15, 2018.